Lunar Tidal Winds Measured in the Upper Atmosphere (78–105 km) at Saskatoon, Canada

R. J. STENING*

High Altitude Observatory, National Center for Atmospheric Research, Boulder, CO 80307

C. E. MEEK AND A. H. MANSON

Institute of Space and Atmospheric Studies, University of Saskatchewan, Saskatoon, Canada

(Manuscript received 7 July 1986, in final form 30 October 1986)

ABSTRACT

Six years of winds data measured by the partial reflection drifts technique have been analyzed for lunar tides. Data are available at 3 km intervals of height and are separately analyzed in two year datasets to check consistency. A month-by-month seasonal variation is derived. Largest amplitudes of the lunar tide occur in January–February with a smaller maximum in summer. The vertical wavelength is longest in summer, and the tide then resembles that predicted for a pure (2, 2) mode. In winter vertical wavelengths range from 25 to 81 km in different years. Several of these results do not agree with the model of Forbes. An O_1 component of the lunar tide could not be detected.

1. Introduction

While there have been many analyses of lunar tides in the geomagnetic variation (Stening and Winch, 1979; Malin, 1973; Schlapp and Malin, 1979) and of other parameters in the ionosphere (Matsushita, 1967), there have been few direct measurements of the lunar tide in the neutral winds in the thermosphere. Matsushita (1962) tabulates some early results from radio fading methods but these could not provide the height structure and seasonal variation which we shall find. Meteor winds measurements by Greenhow and Neufeld (1961) and by Tsuda et al. (1981) were also unable to give the detail which we shall obtain. Some determinations of the lunar tide in winds at ground level have been summarized by Chapman and Lindzen (1970). However, only one of these was well determined and that, at Hong Kong, employed more than 60 years of data. Experience has shown that only two years of data are sufficient for lunar tidal determinations at ionospheric heights.

Since the medium frequency (2.2 MHz) radar has been running continuously at Saskatoon (52°N, 107°W) since mid-1978, a large quantity of data is available for lunar analysis. In this paper data from 1980 to 1985 are used so that several independent determinations of the lunar tide can be made using three different two-year datasets as well as the whole six years together. The lunar tide is much smaller than the solar tides and other wind fluctuations at these heights and some values obtained are of similar magnitude to the errors. If similar results are obtained in different years, then we will have greater confidence in their reliability.

The winds are measured by the partial reflection drift technique using spaced antennas and a full correlation analysis (Gregory et al., 1979; Meek et al., 1979; Meek, 1980). The mean winds, solar tides and other components from the same dataset have been reported by Manson and Meek (1984, 1985, 1986a). A preliminary lunar analysis was made by Meek and Manson (1987).

2. Method of analysis

The dominant term in the lunar tidal potential is M_2 which varies as $\sin 2\tau$, where τ is the mean lunar time and is related to the lunar age ν and local time t by $\tau = t - \nu$. This tide interacts with other periodic atmospheric variations to give other harmonic components. The smaller amplitude O_1 term varies as $\sin(\tau - \nu - h)$ where h is the longitude of the mean Sun. The presence of the O_1 tide in the upper atmosphere will be discussed later.

The lunar tidal analysis was performed using the method of Winch and Cunningham (1972). This is a variant of the Chapman–Miller method extended to include seasonal variations of the lunar tide. Further elucidation of the method is given in Winch (1981). The analysis provides lunar harmonic components of the form

$$l \sin\{nt \pm 2\nu + (k-2)h + \lambda\}$$

* Permanent Address: School of Physics, The University of New South Wales, Kensington 2033, Australia.

where l is the amplitude and $n = 1$ to 4. For example the term $l \sin(2t - 2v - h + \lambda)$ represents part of the annual variation of the lunar semidiurnal tide. The minus sign preceding the $2v$ term indicates a "phase law" tide while the plus sign indicates a "partial tide"; h gives a measure of season, $k = 0$ to 4, and λ is the phase. The partial tides are discarded because they are not generated directly by the lunar gravitational potential and frequently have contributions arising from other sources, such as magnetic disturbances, which on occasion have similar periodicities to the lunar tides. This leaves us with 20 harmonic terms which are then combined to give the semimonthly tide

$$l'(t) \sin\{\lambda'(t) - 2v\} = l_d(t) \sin\{\lambda_d(t) + 2\tau\}$$

where the amplitude l' and phase λ' depend on the local time t. These can then be calculated for various seasons (values of h). The lunar semidiurnal tide has the same amplitude l_d as the semimonthly tide and a phase $\lambda_d = \lambda' - 2t$ (Malin, 1970). The phases will be presented in this work as the value of τ when this tide reaches maximum: $\tau_m = \pi/4 - \lambda_d/2$.

This analysis method requires as input hourly values for each of the 24 hours in each day included. After forming hourly means of the raw wind data, a strategy then had to be devised to fill in gaps in the data so that the analysis could proceed.

The data collected consisted of eastward and northward wind values at virtual heights from 78 to 105 km in 3 km steps during the six years 1980–85. (The two top heights are in the E region so real heights will be less.) These were edited to fill in gaps as follows:

(i) An hourly mean which has been formed from more than one raw velocity measurement is accepted as is. If there is only one velocity measurement in the hour, this value is accepted if it occurs during the day (0900–2000 local time). Otherwise interpolation is attempted in the following order.

(ii) *Time interpolation:* If accepted hourly means are available at both adjacent hours, then the single gap is filled with the average of these.

(iii) *Height interpolation:* If accepted values are available at the two heights just above and below the gap, then the average of these values is inserted in the gap.

(iv) *Daily tidal fit:* If, for a given day, there are 16 or more hours with accepted values, then a harmonic analysis is performed on these values (least squares linear fit of a mean plus 24 and 12 h harmonics). The rms deviation is calculated and the gaps are then filled with the fitted value plus a random error distributed uniformly in the range of ± 1 rms deviation.

(v) *5-day fit:* This is performed in a similar manner to the one-day fit except that values from 5 successive days are used and an harmonic fit is evaluated if there are then 16 or more hours with accepted values.

(vi) *11 day fit:* This is the same as the 5-day fit except that 11 successive days are used.

(vii) If there are still gaps left after all these attempts (about three occurrences in the six years of data), then monthly tidal means are formed over 9 km layers (78–84, 87–93, 96–102 and 105–111 km) and values derived from these, including a suitable random error, are inserted in any remaining gaps.

It should be noted that none of the above procedures is likely to introduce any lunar periodicity into the data.

3. Results

a. Diurnal variation

Figure 1 illustrates the kind of results obtained by the analysis with the amplitude and phase (given as lunar hour of maximum) varying with local time. We are uncertain why there should be any local time vari-

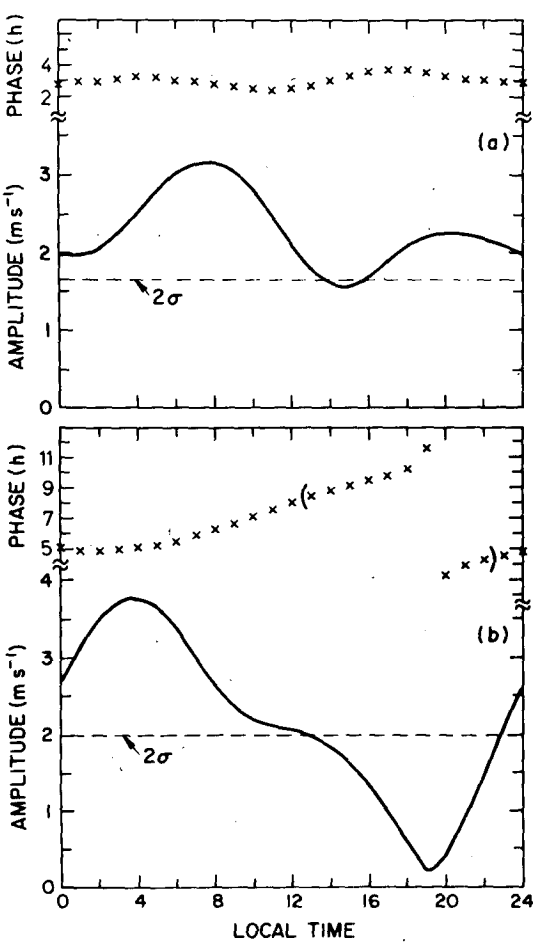

FIG. 1. Diurnal variation of amplitude and phase of lunar winds at 105 km virtual height in May using 6-years dataset. (a) northward winds, (b) eastward. Dashed line indicates 2σ level.

ation of amplitude or phase but find that this often does occur with a tendency towards larger amplitudes in the morning than in the afternoon. We note in passing that lunar analyses of some other parameters also exhibit a diurnal variation, for example the F region critical frequency at Huancayo has a larger lunar tide in the afternoon (Stening, 1986).

Also indicated in Fig. 1 is the level of 2 standard deviations. This corresponds to about 98% confidence. The standard deviation is obtained as the square root of the sum of the squares of all the 20 standard deviations of the harmonic components used in the calculation. Any phases associated with amplitudes below this level may be unreliable. Thus, although the eastward wind in Fig. 1 appears to have a large diurnal variation of phase, those phases between the parentheses in the figure are unreliable, and all the reliable values lie between 4.5 and 8 h. In the case of the northward wind, nearly all the amplitudes are well determined and there is very little phase variation. Whatever is causing the diurnal variation is consistent in the three two-year datasets, each of which gives results varying in broadly similar fashion to those in Fig. 1, though the amplitudes differ—a maximum of 5.7 m s^{-1} for the eastward wind in 1982/83 and only 3.0 m s^{-1} in 1984/85 which is less than 2σ for this dataset.

The annual average lunar tide also possesses a diurnal variation. This is obtained by using only the harmonics with $k = 2$. A lack of diurnal variation would require the $n = 2$ harmonic to dominate the others ($n = 1, 3, 4$). This rarely occurs. The diurnal variation calculated with $k = 2$ only is no smaller (on a percentage basis) than when the seasonal terms are included.

b. *Seasonal variation*

Our experiment measures the virtual height which is simply the time for the radar signal to travel to the point of partial reflection multiplied by the free space velocity. Within the E-region the refractive index of the plasma increases to values greater than unity, causing "retardation" or a slowing down of the wave. The use of the free space velocity in deriving the virtual height thus overestimates the true height and so when the virtual height is 105 km, the true height will be somewhat lower. Below 100 km virtual and real heights are equal.

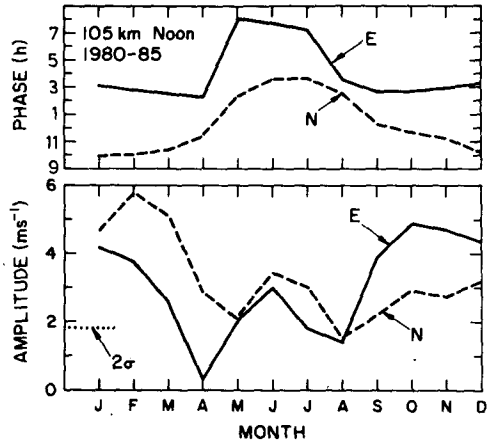

FIG. 2. Seasonal variation of local noon lunar winds at 105 km using 6-years dataset. Full line: eastward winds. Dashed line: northward. Dotted line: 2σ level.

TABLE 1. Largest amplitudes (in m s^{-1}) and months of occurrence.

	Winter		Summer	
	North	East	North	East
1980–81	5.8 Feb	10.0 (night) Jan 8.9 (day) Jan	6.3 (night) June	4.6 (night) June
1982–83	4.5 Mar	6.9 Oct	4.5 July	5.4 (night) May
1984–85	10.3 Feb	7.0 Oct Nov	5.5 June	3.7 June

We shall start at the highest altitude where the variations are more regular and clear cut. The seasonal variation of phase and amplitude is shown in Fig. 2 for an analysis of noon values of all six years of data (2192 days). The plotted points correspond to about the 21st day of each month. There are summer and winter regimes with opposite phases, the winter amplitude being the larger. The northward wind has a large maximum in February while the eastward wind has a broader maximum ranging from September to February. Table 1 is presented to illustrate how much the amplitudes may vary between different years. The winter amplitude in 1984/85 is twice as large as in 1982/83.

The nighttime lunar tide was also examined at 105 km. Figure 3 shows that the seasonal variation is basically similar to that during daytime except that the phase of the eastward wind only varies over about 2 instead of 5 h for the northward wind. In other words in winter day and nighttime phases are similar while in summer there may be about 4 h difference for the eastward wind. This is true also at 102 km but not at 99 km.

At 96 km (Fig. 4) the winter and summer peaks can still be seen with the February peak most pronounced in both wind components. The phases also vary in a similar way to the phases at 105 km but not by as much. The phase difference between February and June for the eastward wind is 2.2 h at 96 km and 5.3 h at 105 km. At this level the nighttime phases do not differ from the daytime phases by more than 2 h when the amplitudes are well determined.

The seasonal variation at 79 km, the lowest height examined, is similar but less distinct (Fig. 5). Amplitudes are smaller and several points are not well determined so the 0600 local time values are also plotted. Here the summer maximum in the eastward winds is

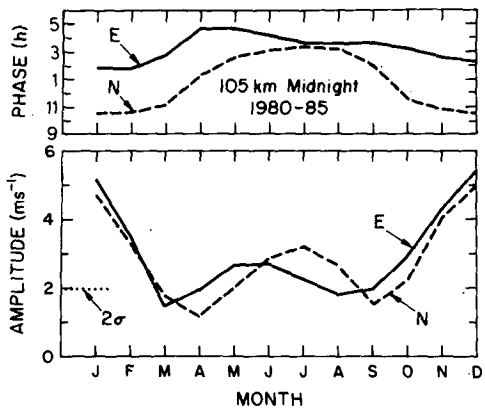

FIG. 3. Seasonal variation of midnight values of lunar winds at 105 km.

more clearly seen. The behavior of the individual two-year datasets is quite variable at this height so no further comment will be made.

c. *Height variation*

In order to make comparisons with models, we have plotted the height variations at solstices and equinox, though we found above that amplitudes frequently maximize in February.

The results using all six years of data are presented in Fig. 6 for December. But before trying to interpret this figure we should look at Fig. 7 where the individual two-year dataset results are plotted. It can immediately be seen that the 1984/85 results differ substantially from the other two, so that combining all three as in Figure 6 does not give a meaningful result. The phases for the earlier years give evidence of a vertical wavelength of about 25 km above 87 km while in 1984/85 the wavelength for the eastward wind is 81 km or more. Around 84 km there is a transition and wavelengths may be longer below this level. In June (Fig. 8) all three datasets give similar results above 93 km, showing a long wavelength. Again there is a transition region near 84 km and this can be seen more clearly in Fig. 8b, where the 0600 local time results are plotted.

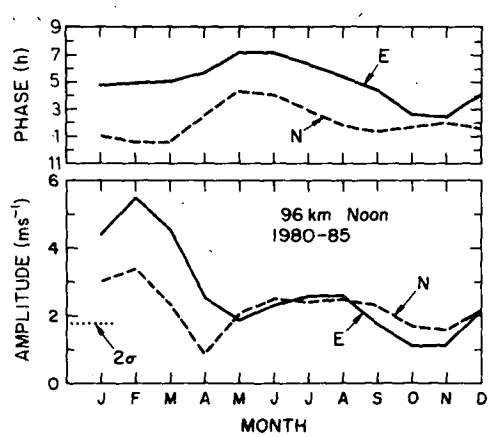

FIG. 4. Seasonal variation of noon values of lunar winds at 96 km.

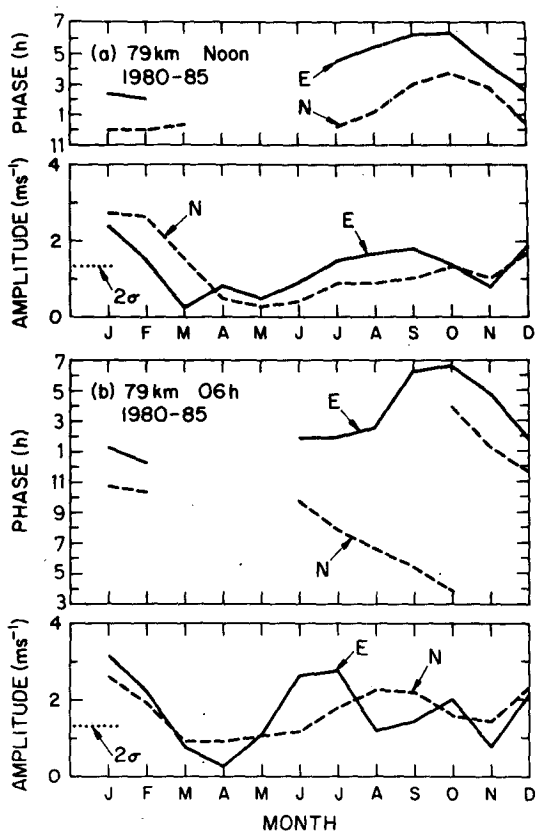

FIG. 5. Seasonal variation of lunar winds at 79 km. (a) noon values, (b) values at 0600 local time.

The March results in Fig. 9 are more variable, as

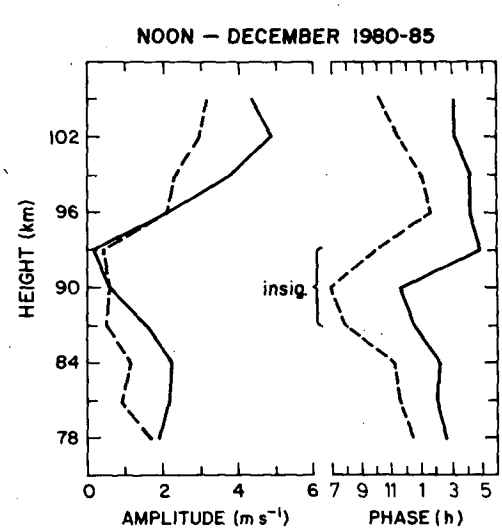

FIG. 6. Variation of phase and amplitude with height of lunar winds at noon in December using 6-years dataset.

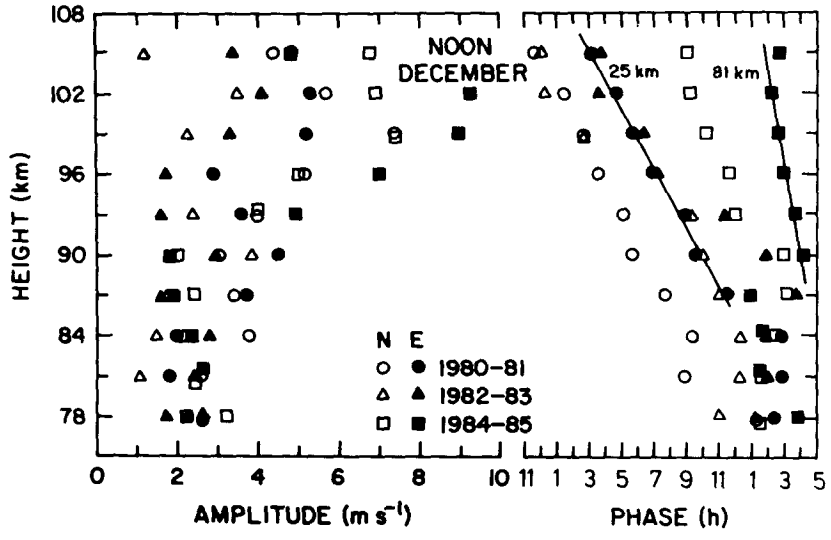

FIG. 7. Variation of noon values lunar winds with height in December. Northward winds have open symbols, eastward filled symbols. 1980/81 circles, 1982/83 triangles and 1984/85 squares.

may be expected. Wavelengths are about 30 to 40 km in the 93–102 km region and agreement between the three datasets is reasonable.

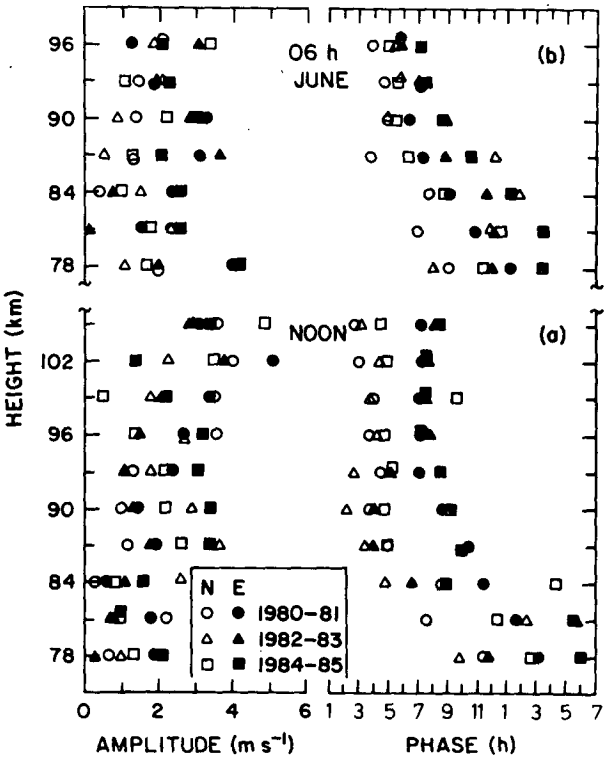

FIG. 8. Variation with height of lunar tidal winds in June (a) noon values, (b) values at 0600 local time in lower height range.

4. Discussion

Previous measurements such as those of Tsuda et al. (1981) and those mentioned by Matsushita (1962) do not have enough information on variation with height and season and so it is difficult to make any comparison with them.

The most recent theory is that of Forbes (1982) and his results taken from Forbes and Gillette (1982) are shown in Fig. 10 for 54° latitude. Looking at amplitudes above 100 km, he finds very large amplitudes (up to 22 m s^{-1}) in summer and smallest amplitudes in winter. While we also find amplitudes $\sim$ 10 m s^{-1} in winter, these are our largest and the summer values are usually smaller. Not only is there a very large difference in the summer amplitudes but the vertical wavelengths are also very different. Forbes obtains about 27 km while our measured summer wavelength (June) is very large, at least at heights above 96 km. In winter sometimes we find a vertical wavelength as short as 25 km, but in other years it may be 81 km. Forbes' winter results also give about 80 km in the 93–100 km region with shorter wavelengths above and below. The picture is more confused at equinox with much discontinuity and year-to-year variability at the lower heights. Above 90 km a vertical wavelength of 30–40 km agrees with Forbes. However, at 96 km we obtain a phase ranging from 5 to 6.5 lunar h for the eastward wind while Forbes has 10.5 h.

In Forbes' model the height of maximum amplitude lies between 107 and 111 km. This is just above the range of our measurements. In December most of our amplitudes maximize at 102 km. In June the maximum is sometimes at 102 km and sometimes higher.

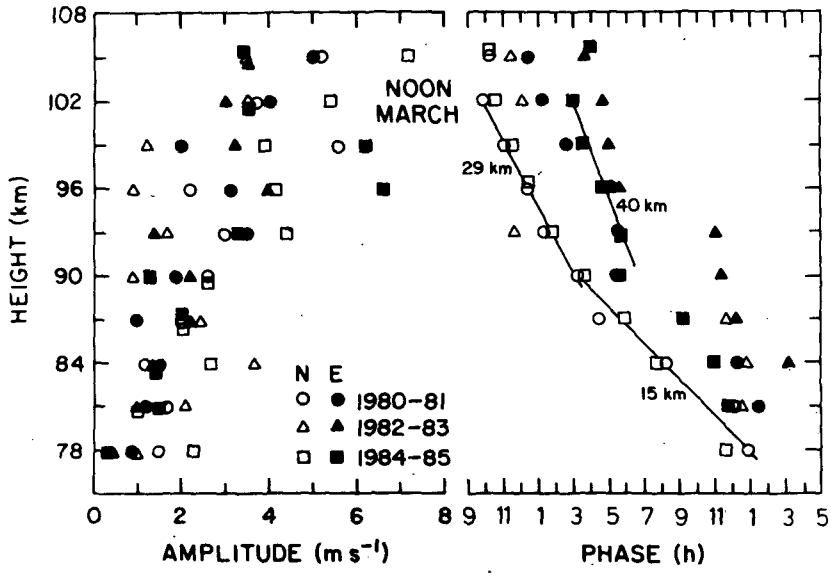

FIG. 9. Variation with height of noon values of lunar tidal winds in March.

So this feature agrees reasonably well with Forbes' model.

Around 81–84 km in our results, there appears to be a transition, often accompanied by minimum amplitudes. In June there is a large phase change in this height region, while in December there is a change from long vertical wavelengths below to short wavelengths above. Similar changes can also be seen in the model results, probably due to mode coupling effects.

Forbes' model produces appreciable (2, 3), (2, 4) and (2, 5) mode amplitudes at and above the heights of our measurements. Our long summer vertical wavelengths may indicate that mode coupling is less effective in that season and our winter results suggest that this effect may have considerable year-to-year variability.

It might be argued that it is inappropriate to compare lunar tides at a certain local time with Forbes' model which refers to a diurnal average. However the main discrepancies, namely (i) December amplitudes larger or similar to June amplitudes and (ii) short vertical wavelengths in December and long in June, are true for all local times. A further check was made by performing the calculation with $n = 2$ components only (i.e., diurnal variations omitted) and these results also support the conclusions.

The behavior of the lunar semidiurnal tide resembles that of the solar semidiurnal tide at Saskatoon in having larger amplitudes and shorter wavelengths in winter than summer (Manson and Meek, 1984, 1985). But the summer regime appears to be shorter for lunar tides,

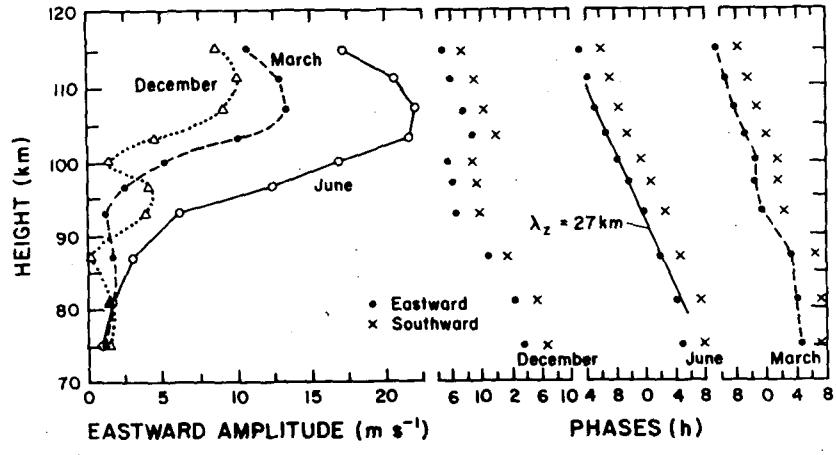

FIG. 10. Theoretical height profiles of lunar semidiurnal winds taken from Forbes and Gillette (1982). Amplitudes are given for eastward winds only. For the phase plots dots are eastward and crosses southward winds.

lasting from May to July or August only. For the solar semidiurnal tide the summer phase values begin about the same time (April–May), but the phases do not change back again until after October (Manson and Meek, 1984). These differences might be explained by seasonal changes in the ozone concentration which controls the forcing function of the solar tides. The lunar gravitational forcing function has very little seasonal change and so the observed variation must be due to changes in the mean winds or the atmospheric temperature profile through which the tide propagates.

We should be concerned to ask whether the lunar tides reported here might not be caused by a modulation of the solar tides by magnetic activity with a periodicity near 14 days. Manson and Meek (1986b) have shown that there is an effect of magnetic activity on the solar semidiurnal tidal amplitude but it is small. Furthermore there is no reason to expect any effect induced by magnetic activity to have a similar lunar phase from year to year (as our June results do). We are therefore confident that contamination by magnetic disturbance effects is minimal.

The summer solar eastward wind semidiurnal phase determined by Manson and Meek (1985) (7 h) was found to agree with that predicted for the (2, 2) mode by Chapman and Lindzen (1970). The summer lunar semidiurnal phase measured at 96 km is 7.8 h while that given by Chapman and Lindzen is about 4 h, suggesting that the simple theory derived from the (2, 2) mode alone is not completely adequate during summer. It has been remarked earlier (Manson and Meek, 1985) that the mean summer westward winds in Forbes' model are not as intense as those observed in the 80 km region and this may explain the difference between predicted and observed modes. The longer wavelength observed in the winter 1984–85 data makes one ask whether there was any difference in the mean flow during these years. In fact, in December 1984 the mean winds measured at Saskatoon were weaker in the 60–70 km region while the solar tides at this time were similar to other years. Further global or hemispheric data will need to be examined before any relationship can be established.

The occurrence of the maximum amplitude in February, as found at 105 km, has also been noted in lunar geomagnetic variations by Stening and Winch (1979) and by Schlapp and Malin (1979). Both of the latter investigations also found phase anomalies in the lunar geomagnetic tide in local winter and suggested this may be due to the failure of the lunar dynamo in the winter hemisphere, the currents being driven by electric fields generated in the summer hemisphere and communicated to the winter hemisphere along the magnetic field lines. Although this effect was not observed in the North American sector, the present results showing the largest amplitude in winter suggest that this may not be the correct explanation. On the other hand, the shorter vertical wavelength wind in winter is much less efficient in generating electric currents, so the summer lunar dynamo may still predominate. We also suggest that the presence of antisymmetric modes may be responsible for these phase anomalies, but calculations are necessary to confirm this.

Is there an O_1 tide present? The discussion so far has implicitly assumed that the lunar tide is basically semidiurnal varying as $\sin 2\tau$. This assumption is justified by the calculations of Geller and Schoeberl (1973) who found the diurnal O_1 tide to have an amplitude of only about 1% of the M_2 tide at 100 km. However, Tsuda et al. (1981) claim to have measured an O_1 tide in the northward wind at 100 km which is nearly twice as large as the M_2 tide. We will therefore examine our data for traces of the O_1 tide.

The O_1 tide varies as

$$\sin(t-2\nu-h)=\sin(\tau-\nu-h)$$

so that it also has a semimonthly variation 2ν, but a solar diurnal variation t. The phase varies with season h. Schlapp (1977) has pointed out that a mixture of M_2 and O_1 tides should give a circle when values at a particular solar hour are plotted on a dialgram with respect to season as in Fig. 11. The M_2 tide (assumed constant with season) is the vector from the origin to the center of the circle while the O_1 tidal amplitude is the radius of the circle. The 96 km results in Fig. 11a appear to fit this picture, but a seasonal change in the M_2 tide can produce similar results. A pure O_1 tide has a different phase change with solar hour. In our analysis the lunar time of maximum amplitude τ_m would be constant for a pure M_2 tide and would change by 0.5 lunar hours for every solar hour for a pure O_1 tide. Examination of the analysis results shows that $\Delta\tau_m/\Delta t$ varies from -0.05 to -0.18 for the almost circular dialgram at 96 km, so that this must be due to a seasonal variation in M_2. At greater heights the circle degenerates almost into a straight line, indicating a seasonal variation of M_2 and absence of O_1.

In cases where there appears to be an appropriate diurnal variation of phase (such as in part of Fig. 1 for eastward winds) the seasonal dialgram in Fig. 12 does not show that form which suggests the presence of an O_1 component. We therefore feel confident in our interpretations based on the absence of any significant O_1 tide.

As a further check we performed the analyses using only the diurnal Fourier coefficients and only the semidiurnal coefficients. The circle in Fig. 11 did not appear when only diurnal coefficients were used. Furthermore this and many other results using diurnal coefficients had amplitudes less than 2σ at all seasons. The semidiurnal results, on the other hand, yielded phases very similar to the full analysis first described but the amplitudes were sometimes different, though peaks were generally at similar seasons.

Manson and Meek (1984, 1985) have shown that the solar diurnal tidal amplitudes may reach 20 m s^{-1}

and the semidiurnal tides 30 m s^{-1}. At some altitudes these magnitudes are similar to the mean winds and it is through this background of solar tides that the lunar tide must propagate. It seems reasonable to suggest that the diurnal changes in lunar tidal amplitude reported here may be due to interactions with these solar tides. Models, such as that of Forbes (1982), so far only have a background of mean winds.

5. Conclusions

1) The lunar tidal winds have been measured at Saskatoon and have been shown to exhibit considerable seasonal, year-to-year and possibly diurnal variation.

2) Amplitudes are generally largest in January–February with a smaller maximum in summer. This variation is opposite to the model of Forbes (1982).

3) The vertical wavelength is generally long in summer suggesting the presence of a pure (2, 2) mode.

4) Vertical wavelengths may vary from 25 to 81 km in winter indicating varying amounts of mode coupling in different years.

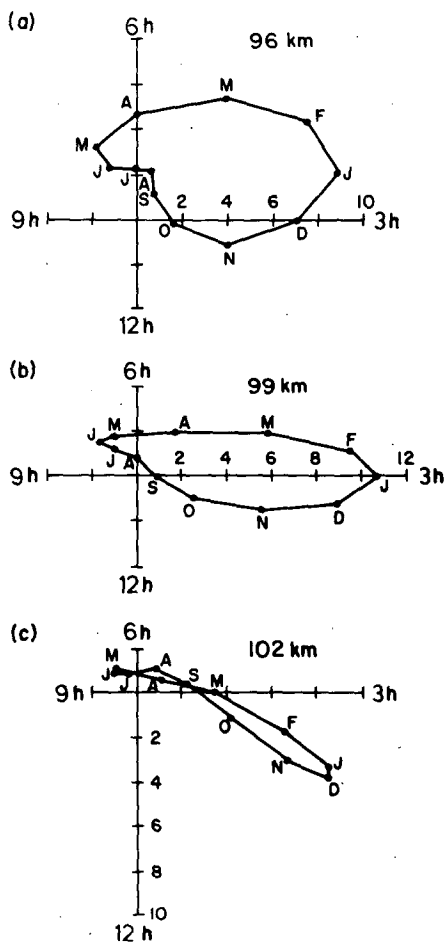

FIG. 11. Dialgram depicting monthly variation of eastward lunar wind at noon. Amplitudes in m s^{-1}, phases are lunar hours of maximum, 1984/85 dataset.

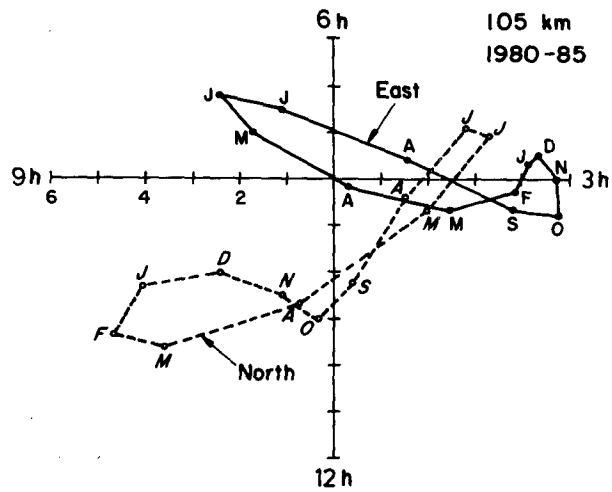

FIG. 12. Monthly variation of noon lunar winds at 105 km using 6-years dataset.

5) No significant O_1 tide was detected.

6) After finding such large winter amplitudes, the phase anomalies in the lunar geomagnetic tide may not be explained by the failure of the lunar dynamo in winter although its shorter wavelength makes it less efficient. An alternative explanation may be the presence of antisymmetric modes.

Acknowledgments. The financial support of the Natural Science and Engineering Research Council and the Atmospheric Environment Service, both of Canada, is gratefully acknowledged; also of the Institute of Space and Atmospheric Studies, through the University of Saskatchewan, Saskatoon. R. Stening thanks A. D. Richmond for a critical review of the manuscript and the High Altitude Observatory of the National Center for Atmospheric Research for a Visiting Scientist appointment. Some of the computer programs used here were originally written by D. E. Winch and his assistance is gratefully acknowledged. The National Center for Atmospheric Research is sponsored by the National Science Foundation.

REFERENCES

Chapman, S., and R. S. Lindzen, 1970: *Atmospheric tides,* D. Reidel.

Forbes, J. M., 1982: Atmospheric tides. 2. The solar and lunar semidiurnal components. *J. Geophys. Res.,* **87,** 5241–5252.

——, and D. F. Gillette, 1982: A compendium of theoretical atmospheric tidal structures. Part 1: Model description and explicit structures due to realistic thermal and gravitational excitation, Air Force Geophysics Laboratory Rep. AFGL-TR-82-0173 (1), Hanscom AFB, MA.

Geller, M. A., and M. R. Schoeberl, 1973: *Rev. Italinia Geofis.,* **22,** 379–384.

Greenhow, J. S., and E. L. Neufeld, 1961: Winds in the upper atmosphere. *Quart J. Roy. Meteor. Soc.,* **87,** 472–489.

Gregory, J. B., C. E. Meek, A. H. Manson and D. G. Stephenson, 1979: Developments in the radiowave drifts technique for measurement of high altitude winds. *J. Appl. Meteor.,* **18,** 682–691.

Malin, S. R. C., 1970: Separation of lunar daily geomagnetic variations into parts of ionospheric and oceanic origin. *Geophys. J. Roy. Astronom. Soc.*, **21,** 447–455.

——, 1973: Worldwide distribution of geomagnetic tides. *Phil. Trans. Roy. Soc. London,* **A274,** 551–594.

Manson, A. H., and C. E. Meek, 1984: Winds and tidal oscillations in the upper middle atmosphere at Saskatoon (52°N, 107°W, L = 4.3) during the year June 1982–May 1983. *Planet. Space Sci.*, **32,** 1087–1099.

——, and ——, 1985: Middle atmosphere (60–110 km) tidal oscillations at Saskatoon, Canada (52°N, 107°W) during 1983–1984. *Radio Sci.*, **20,** 1441–1451.

——, and ——, 1986a: Dynamics of the middle atmosphere at Saskatoon (52°N, 107°W): A spectral study during 1981, 1982, Rep. 1, 1986, Atmos. Dyn. Group, Inst. of Space and Atmos. Stud., University of Saskatchewan, Saskatoon, Canada.

——, and ——, 1986b: Comparisons between neutral winds near 100 km at Saskatoon (52°N, 107°W) and variations in the geomagnetic field (1979–1983), Report No. 2., 1986, Atmos. Dyn. Group, Inst. of Space and Atmos. Stud., University of Saskatchewan, Saskatoon, Canada.

Matsushita, S., 1962: Lunar tidal variations of sporadic E. *Ionospheric Sporadic E,* E. K. Smith and S. Matsushita, Eds., 194–214, Pergamon, Oxford.

——, 1967: Lunar tides in the ionosphere. *Handbook of Physics,* **49,** 547–602.

Meek, C. E., 1980: An efficient method for analyzing ionospheric drifts data. *J. Atmos. Terr. Phys.*, **42,** 835–839.

——, and A. H. Manson, 1987: *J. Atmos. Terr. Phys.*

——, —— and J. B. Gregory, 1979: Internal consistency analyses for partial and total reflection drifts data. *J. Atmos. Terr. Phys.*, **41,** 251–258.

Schlapp, D. M., 1977: Lunar geomagnetic tides and the ocean dynamo. *J. Atmos. Terr. Phys.*, **39,** 1453–1457.

——, and S. R. C. Malin, 1979: Some features of the seasonal variation of geomagnetic lunar tides. *Geophys. J. Roy. Astronom. Soc.*, **59,** 161–170.

Stening, R. J., 1986: Lunar effects in the F region of the ionosphere. *J. Geophys. Res.*, **91,** 4581–4584.

——, and D. E. Winch, 1979: Seasonal changes in the global lunar geomagnetic variation. *J. Atmos. Terr. Phys.*, **41,** 311–323.

Tsuda, T., J. Tanii, T. Aso and S. Kato, 1981: Lunar tides at meteor heights. *Geophys. Res. Lett.*, **8,** 191–194.

Winch, D. E., 1981: Spherical harmonic analysis of geomagnetic tides 1964–65. *Phil. Trans. Roy. Soc. London,* **A303,** 1–104.

——, and R. A. Cunningham, 1972: Lunar magnetic tides at Watheroo: seasonal, elliptic, evectional, variational and nodal components. *J. Geomag. Geoelec.*, **24,** 381–414.